

## Supporting Information

### **Facile Preparation of Ductile, Free-Standing and Multilayer Polymeric Optical Data Storage Media with Macroscopic Structural Homogeneity**

*Yang Feng,<sup>ab</sup> Jingfa Yang,<sup>a</sup> Jiang Zhao<sup>\*a</sup> and Guangming Chen<sup>a</sup>*

<sup>a</sup> Beijing National Laboratory for Molecular Sciences, Institute of Chemistry, Chinese Academy of Sciences, Beijing 100190, P. R. China.

\*E-mail: jzhao@iccas.ac.cn

<sup>b</sup> University of Chinese Academy of Sciences, Beijing 100049, P. R. China

### **1. Preparing PC/fluorophore layer on PI film**

A PI film with a thin PC/fluorophore layer attached on its surface is very important for the following hot pressing procedure. Any method, as long as it can be used to make a thin PC/fluorophore layer on PI film, is compatible with our sample preparation protocol.

The sandwiching method in this study is a demonstration of preparing PC/fluorophore layer on PI film. By controlling the concentration of PC and the pressure to sandwich the PC/fluorophore/THF layer, the thickness of PC/fluorophore layer can be controlled to some extent, but to better control the layer thickness could need other methods.

Spin-coating should be the most favored method of acquiring PC/fluorophore layer on PI film surface, however, the spin-coating device for laboratory use is very primitive and not suitable for making thin films with big size, and moreover, the PI film is too soft to be fixed on the primitive spin-coating device as substrate. Therefore, the sandwiching method was chosen instead. If dedicated device is available, spin-coating could be very helpful in making thinner PC/fluorophore layer with better controlled thickness.

### **2. Control the thickness of neat PC film**

The thickness of neat PC film is important, as it determines the distance between two adjacent photosensitive layers in the multilayer structure.

Currently, the neat PC films were acquired at 230 °C, 10 MPa, and under such condition the thickness of neat PC films cannot be made thinner than ~50 μm. To acquire thinner films, higher temperatures (e.g., 300 °C) are preferred. Unfortunately, the rubbery seal ring in the vacuum chamber of our compression apparatus will be damaged at higher temperatures. Note that compression under vacuum is necessary for preparing PC and many other polymer films, or there will be bubbles left within the film.

### **3. Diffusion of fluorophores after hot pressing**

Secondary ion mass spectroscopy (SIMS) analysis was first applied to evaluate the diffusion of fluorophores from PC/fluorophore layer to neat PC layer after hot pressing. The fluorophore is BODIPY 650/665, which has characteristic elements including B and F. The analysis started from the top PC/fluorophore layer to the lower neat PC layer. Ar<sup>+</sup> was chosen as primary ion to detect the element B – as shown in Fig. S1a, although the signal is weak, the trend for element B is clearly different with those of C and H. As the sputter time increases, the intensities of C and H are nearly constant while the intensity of B continuously decreases. The element F was

detected by applying  $\text{Cs}^+$  as primary ion, and result (Fig. S1b) also shows that the intensity of F continuously decreases as the intensities of other elements (C, H and O) remain nearly constant. Due to low  $\text{Cs}^+$  energy and relatively thick PC/fluorophore layer (in micron scale), the SIMS analysis of F took nearly 5 h (including sputter time (nearly 2000 s) and charge compensation) and was stopped afterwards due to time limit. Based on the results of B and F, it is reasonable to deduce that the distribution of fluorophores after hot pressing can be illustrated in Fig. S2 – due to hot pressing, part of fluorophores in the original PC/fluorophore layer diffused into neat PC layer.

The SIMS instrument does not have depth measuring accessory, so we tried the EDS analysis on the cross section of the film with an SEM/EDS microscope system. However, no signals of the organic fluorophores were detected and it might be because that the fluorophores are composed of light elements and not suitable for EDS analysis. We further used inorganic fluorophores (CdSe/ZnS quantum dot in this analysis) instead, but still no signal could be acquired. It seems that the EDS analysis needs much higher fluorophore concentration than fluorescence imaging does to generate strong signals.

Currently, we could only roughly evaluate the diffusion depth of fluorophores through confocal microscopic imaging. As shown in Fig. S3, the confocal image on the right coincides with the schematic on the left, and the fluorophore (BODIPY 650/665) concentration decreases as it goes deeper (Z-axis) into the film. The thickness of the initial PC/fluorophore layer prepared by sandwiching method is 5-6  $\mu\text{m}$ , judging from the confocal image, the diffusion depth of fluorophores after hot pressing could be 0.5-2  $\mu\text{m}$ . Since the resolution of confocal imaging in thickness (Z) direction is relatively limited, and the fluorophore concentration gradually decreases inside the film, it is hard to more accurately calculate the fluorescent layer thickness after hot pressing.

It is envisioned that the final thickness of the fluorescent layer after hot pressing can be optimized by reducing the initial PC/fluorophore layer thickness (i.e., counteract the fluorophore diffusion).

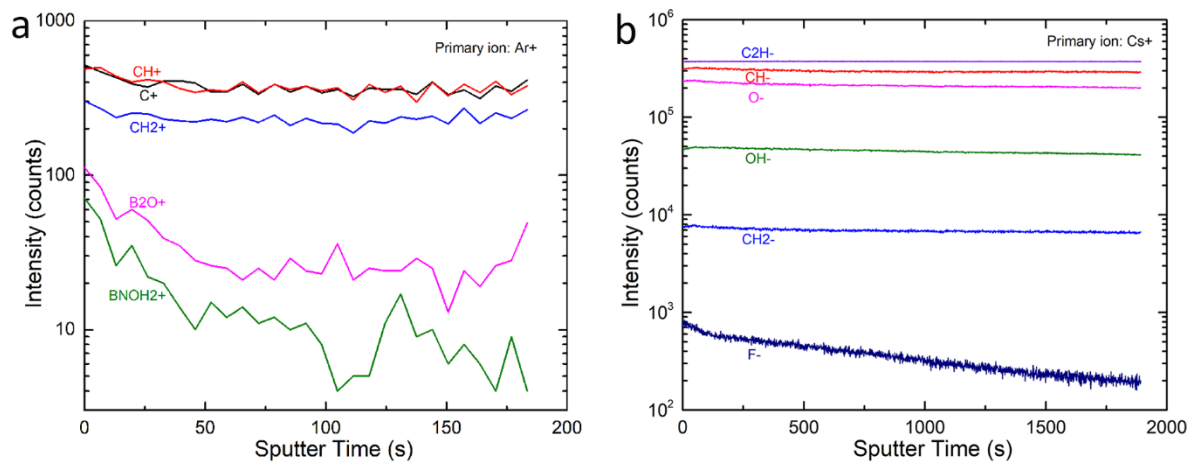


**Fig. S1** SIMS analysis results of the distribution of BODIPY 650/665 after hot pressing. (a) Element B. (b) Element F.

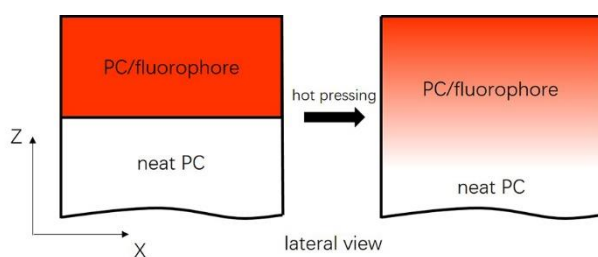


**Fig. S2** Schematic illustration of the fluorophore diffusion within PC film after hot pressing (lateral view).

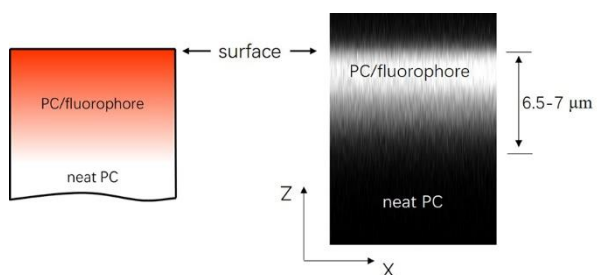


**Fig. S3** Fluorophore distribution within PC film captured by confocal fluorescence microscopy (lateral view).

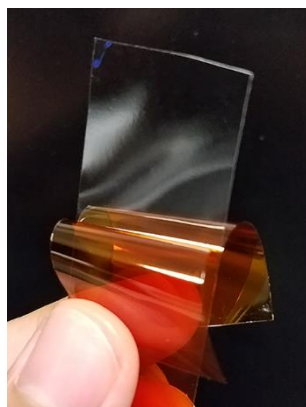


**Fig. S4** Free-standing PC film with fluorescent layer embedded, which is prepared with the present method.

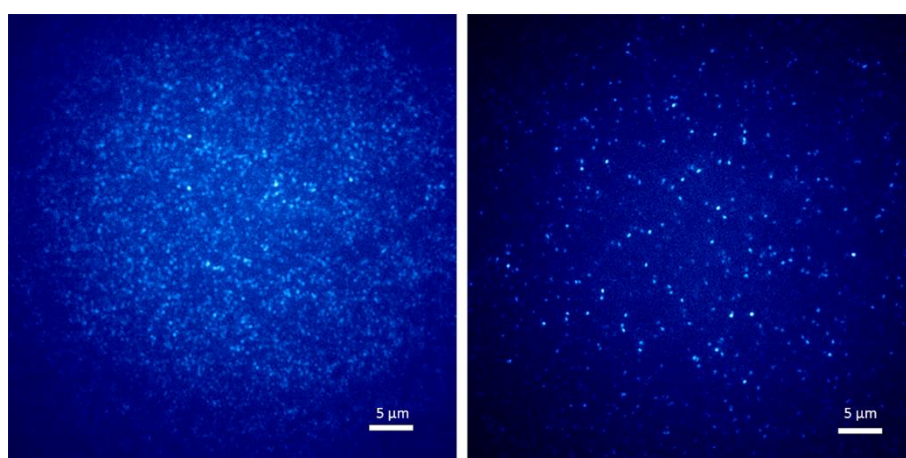


**Fig. S5** Wide-field fluorescence microscopic images of the fluorescent layers (ATTO 647N, 639 nm) embedded within PC films ( $\sim 90 \mu\text{m}$ ). With the present preparation method, the fluorophore concentration can be easily tuned.

#### **4. Control experiments of embedding fluorescent layer within PC matrix**

To incorporate a fluorescent layer into PC matrix, the initial idea (Fig. S6a) is to distribute the PC-free fluorophore/cyclohexane solution (PC is insoluble in cyclohexane) evenly on the surface of a PC film by spin coating or solution casting, and then, after the quick evaporation of cyclohexane, cover the previous PC film with another one followed by hot pressing ( $\sim 180 \text{ }^\circ\text{C}$ ) under vacuum. Unfortunately, after being exposed in atmosphere, the fluorophores (especially the inorganic nanocrystals such as quantum dots/rods) could easily lose the fluorescent ability by heating at high temperatures. As a result, the samples made by hot pressing showed very poor fluorescent activity under the microscope. Before hot pressing, we tried to keep the sample-to-be-pressed in the chamber at room temperature, and only started the hot pressing procedure after the chamber was basically vacuum, but the fluorophores still could not survive. Another idea as illustrated in Fig. S6b came up afterwards. The only difference between Fig. S6a and b is that the solvent was switched from cyclohexane to tetrahydrofuran (THF), and PC

is highly soluble in THF. As shown in Fig. S6b, after the fluorophore/THF solution was dropped onto the surface of the PC film, part of the PC near the surface was dissolved by THF as well. Surprisingly, some of the fluorophores survived after the hot pressing procedure and showed decent fluorescent intensity under the microscope. The reason is that some fluorophores can be wrapped by the dissolved PC matrix, thus being isolated completely with the atmosphere. Nonetheless, there are flaws in the second idea. Since part of the PC close to the film surface can be dissolved, the fluorophores could no longer be distributed evenly as a flat layer on the surface (Fig. S6b). Moreover, not all fluorophores could be protected by the dissolved PC. Given that the dissolved PC could protect the fluorophores against high temperature, the final and effective method was proposed and shown in Fig. 1a.

We tried different kinds of commercial fluorophores such as organic ATTO 647N, Alexa Fluor 647, BODIPY 650/665 and several inorganic quantum dots/rods from different companies, and after applying our method in Fig. 1a (i.e., PC/fluorophore layer was first prepared before hot pressing to protect the fluorophores), improvements did exist. However, we do not exclude the possibility that some photosensitive molecules/nanoparticles could be highly stable under hot pressing condition and might not need the protection of PC matrix, but our method is still compatible.

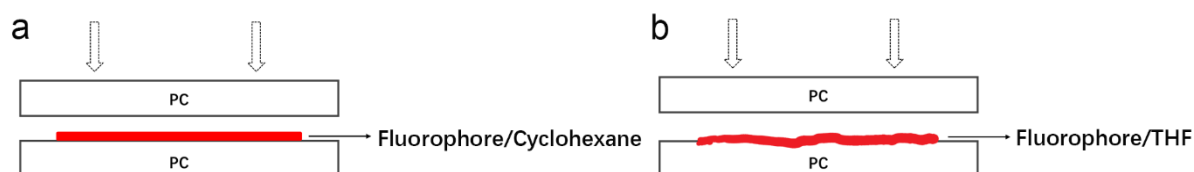


**Fig. S6** Schematic illustration of sample preparation methods (control) in lateral view. (a, b) Fluorophores are dispersed in cyclohexane and THF, respectively. Cyclohexane represents the solvents in which the polymer matrix cannot be dissolved, while in solvents such as THF the polymer matrix is highly soluble.

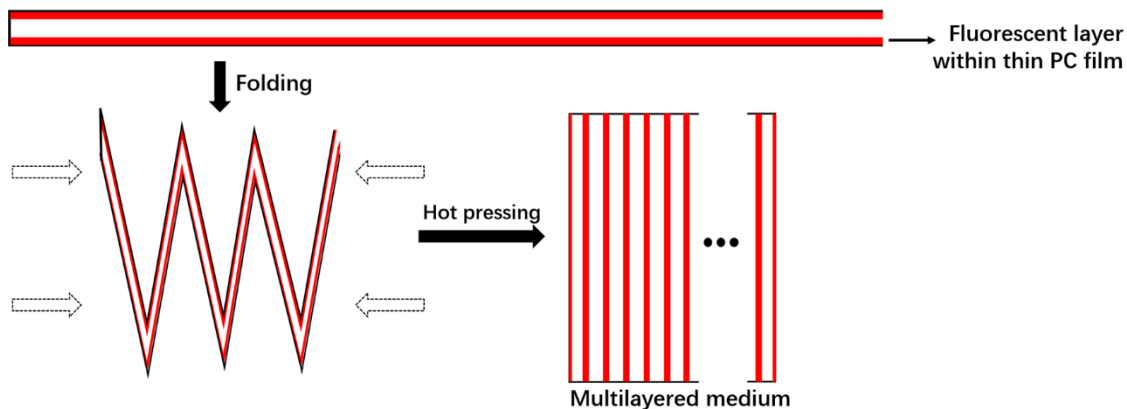


**Fig. S7** Schematic illustration of a candidate route for mass producing multilayered optical data storage materials with macroscopic structural homogeneity (lateral view).

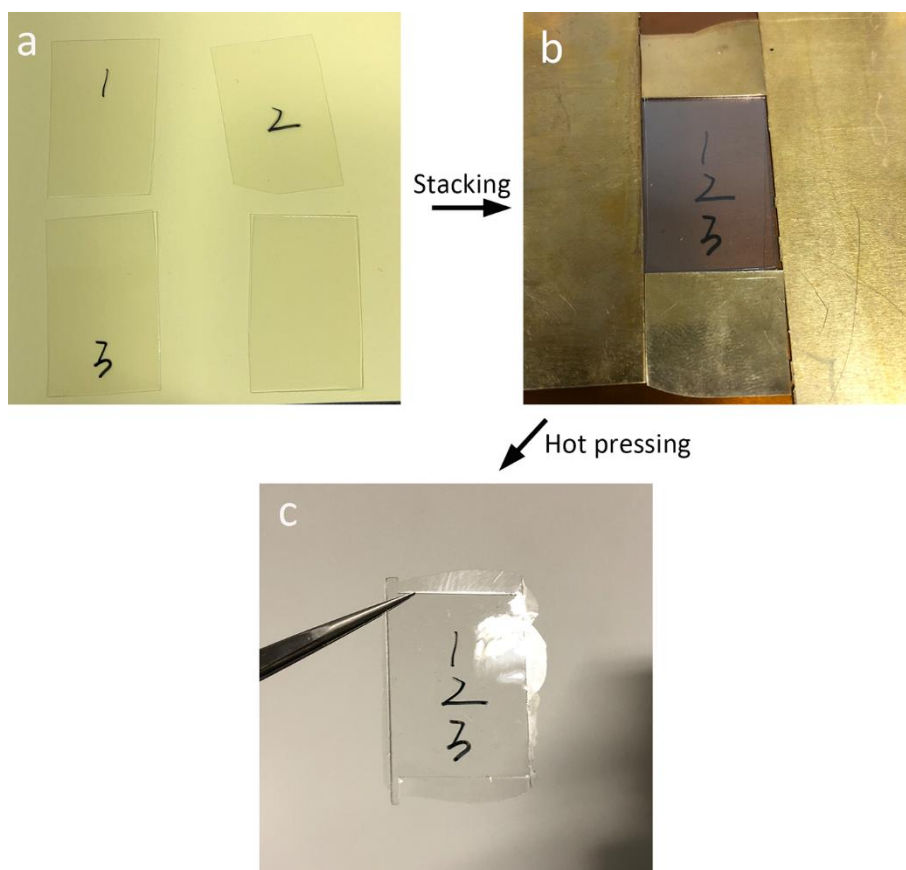


**Fig. S8** Four PC films are stacked and hot pressed to acquire one film with macroscopic homogeneity. (a) Three PC films are marked with sequence numbers on their upper surfaces, and the last film is left blank. (b) Four PC film are stacked based on the sequence numbers (No.1 at the bottom, and No.3 covered by the blank film) and surrounded by spacers. (c) After hot pressing, a film with three sequence numbers (representing different layers) embedded is acquired, and the film shows good transparency and structural homogeneity.

## 5. Compatible bulk samples for wide-field single molecule fluorescence microscopy

To conduct single-molecule fluorescence microscopic studies on bulk samples, simply increasing the sample thickness (e.g., from 100 nm to 100  $\mu\text{m}$ ) is not enough. The background fluorescence has always been a major concern in single-molecule experiments, and it is intrinsic to many polymers or, in other cases, results from the impurities and additives which are difficult to eliminate.<sup>1-3</sup> If the sample thickness is changed from 100 nm to 100  $\mu\text{m}$ , the intensity of the background fluorescence would be much higher. Moreover, for ultra-thin films, the fluorescent probes (i.e., fluorophores) can be distributed in the whole thickness range, but for a 100-micrometer thick film, when the probes are still distributed in the whole thickness range, under the microscope not only the probes in or near the focal plane but also those across the whole light path would be excited, and as a result one can see nothing but a big bright spot in the view field through the microscope (Fig. S9). To overcome this problem, the fluorescent probes within the bulk samples need to be distributed as a thin layer parallel to the film surface, thus controlling the thickness range of excitation.

Since the concentration of the fluorescent probes needs to be very low (nM) for single-molecule microscopy, the background fluorescence of bulk sample could be overwhelming. In our imaging experiments, excitation lights of long wavelength were applied to diminish the background fluorescence, thus relatively enhancing the signal of organic dye molecules (639 nm for ATTO 647N in our work, see Fig. S5). As for inorganic quantum dots/rods, their fluorescence intensity is high enough so that short wavelength excitation lights (e.g., 532 nm) can be used with no problem.

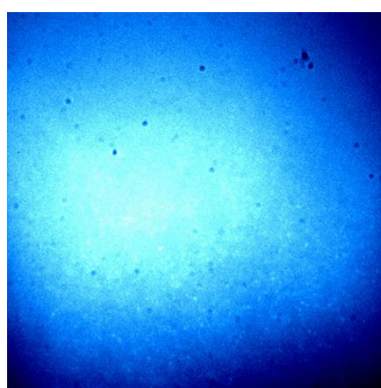


**Fig. S9** Wide-field fluorescence microscopic image of a PC film ( $\sim 80 \mu\text{m}$ ), within which the fluorophores (perylene orange) are distributed across the whole thickness range.



## 6. Details of the wide-field defocused imaging method

As shown in Fig. S10a, to acquire a defocused image, one needs to deliberately move the objective over a short distance  $d$  away from the best focus position, then the defocused image of a fluorophore will show a specific pattern which can be used to determine both the in-plane ( $\phi$ ) and out-of-plane ( $\theta$ ) orientation of the fluorophore (emission dipole). When the fluorophore is oriented parallel to the substrate, a dark line can be seen in the middle of the defocused pattern (see the first row in Fig. S10b,  $\theta \sim 90^\circ$ ), and its direction indicates the in-plane orientation ( $\phi$ ) of the fluorophore. If the fluorophore orientation is out of plane, the dark line in the middle of the defocused pattern will gradually diminish as the  $\theta$  decreases, and only circles can be seen at last. More technical details about the defocused imaging can be found in references.<sup>4,5</sup>

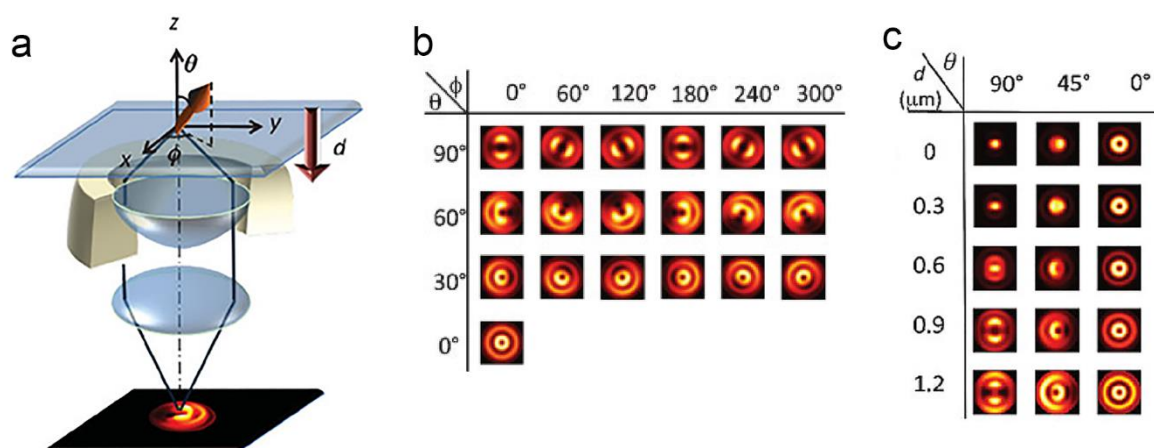


**Fig. S10** (a) Schematic illustration of basic experimental setup for defocused imaging. The tilted arrow on the top represents the spatial orientation of the fluorophore emission dipole. (b, c) Calculated defocused patterns for different (b) in-plane ( $\phi$ ) and out-of-plane ( $\theta$ ) orientations and for (c) different defocusing depths  $d$ . (a, b and c) are reproduced from reference.<sup>4</sup>

The quantum rod used in our work is elongated CdSe/CdS core/shell nanoparticle covered by a thin layer of organic ligands, which stabilize the particle and account for the solubility in either non-polar or polar solvents.

The rubbing treatment with a velvet cloth (Fig. 2c) could inevitably bring impurities (e.g., dust) onto the spin-casted film, thus resulting in severe fluorescence background and adding strong noise to imaging. The quantum rods were chosen to overcome the fluorescence background because they are much brighter than organic fluorophores.

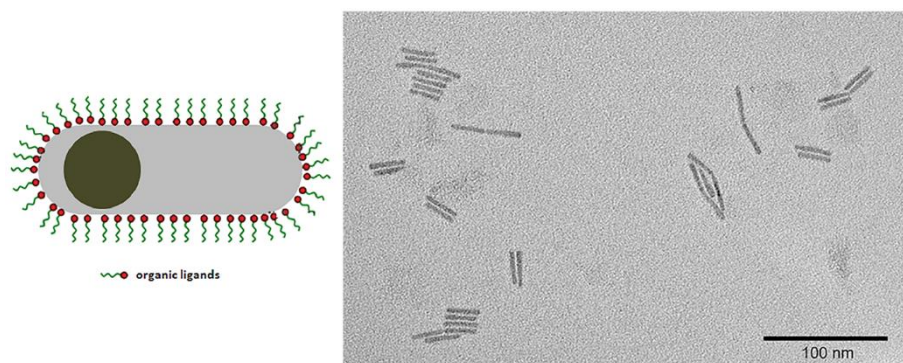


**Fig. S11** Schematic illustration and TEM image of the quantum rod (elongated CdSe/CdS core/shell particle). The dominant transition moment is along its long axis.

## **7. The importance of single-molecule defocused imaging technique in studying polymer mechanical behaviors**

The nonlinear deformation behavior of polymer glasses has always been a major topic in polymer physics research. For the past several decades, many models were proposed to describe the enhanced segmental mobility during deformation, and molecular dynamics computer simulations have directly demonstrated that the molecular mobility in polymer glasses is enhanced. Besides, there have been many experimental attempts to quantify the deformation induced mobility, however, all of them can be categorized into ensemble averaging method, and the local dynamics information is averaged. Therefore, the single-molecule microscopy offers an opportunity to more thoroughly investigate the heterogeneous dynamics of the deforming polymer glass.

## **8. Two mechanical experiments (DMA and tensile fracture test) to further demonstrate the macroscopically homogeneous structure**

### *1. DMA*

As shown in Fig. S12, the analysis was conducted on two kinds of films including one neat PC film ( $\sim 320 \mu\text{m}$ ) and one film ( $\sim 300 \mu\text{m}$ ) acquired by stacking and hot pressing four PC films with fluorophore layers embedded. Results indicate that the mechanical response of the film acquired by stacking and hot pressing shows no obvious difference with the neat PC film. This is understandable because the amount of PC is overwhelming compared to that of fluorophores, and there is no problem in compatibility between adjacent PC layers.

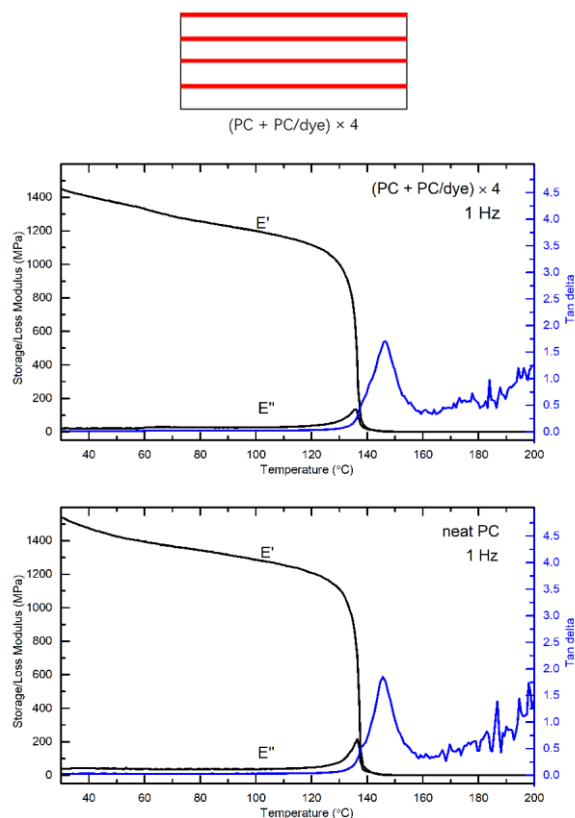


**Fig. S12** DMA results of a neat PC film ( $\sim 320 \mu\text{m}$ ) and a film ( $\sim 300 \mu\text{m}$ ) acquired by stacking and hot pressing four PC films with fluorophore layers embedded.

## 2. Tensile fracture test

As shown in Fig. S13, three polymer films in the sequence of PC-PS (polystyrene)-PC were stacked and hot pressed at  $180 \text{ }^\circ\text{C}$  under vacuum, and the acquired film show good transparency. However, during deformation test, the sandwiched PS layer was broken first, and this is because PS is a brittle polymer which has no yielding behavior (i.e., broken before yielding). At last, due to different mechanical response between PS and PC, layer separation could be clearly seen at the fracture position. As comparison, the film acquired by stacking and hot pressing three PC layers (PC-PC-PC) showed good macroscopic homogeneity.

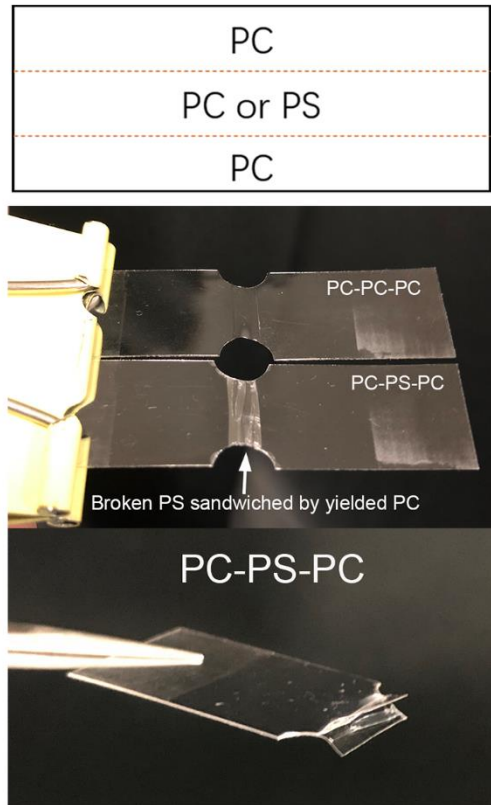


**Fig. S13** Tensile fracture results of two films acquired by stacking and hot pressing specific polymer films in the sequence of PC-PS-PC and PC-PC-PC, respectively.

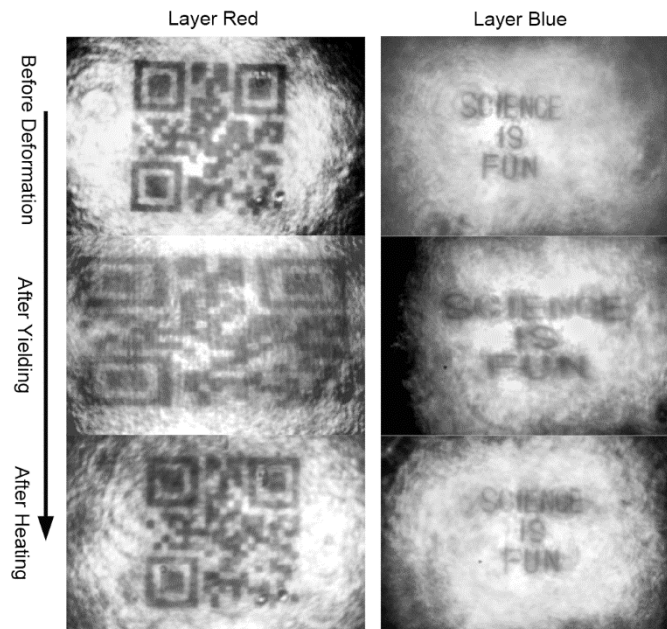


**Fig. S14** Wide-field fluorescence microscopic images of two embedded recording layers (shown in Fig. 5) captured in sample deformation and recovery test.

## 9. Detailed explanation about the proposed hexadecimal format

The hexadecimal format is proposed on the premise that the tiny shaped patterns can be clearly captured by the CCD/CMOS camera, so that subsequent image recognition based on a certain algorithm can be conducted to distill the information. Therefore, the size of tiny shaped

patterns depends on the resolution/definition of the image captured by the camera. Higher resolution/definition means more details per unit area, so that the shaped patterns with smaller size can be recorded (i.e., more patterns can be recorded in a certain area). The data recording density of the binary and hexadecimal code could be roughly evaluated as follows:

Assuming both binary dots and hexadecimal patterns are recorded on the recording layer with the highest density the recording equipment could achieve, as shown in Fig. S15, the minimum distance between adjacent binary dots or hexadecimal patterns is  $d$ , the total recording area is  $A$ , and the number of binary dots and hexadecimal patterns in the total recording area are  $n_B$  and  $n_H$ , respectively. Since a hexadecimal pattern consumes more area than a binary dot,  $n_B > n_H$ .

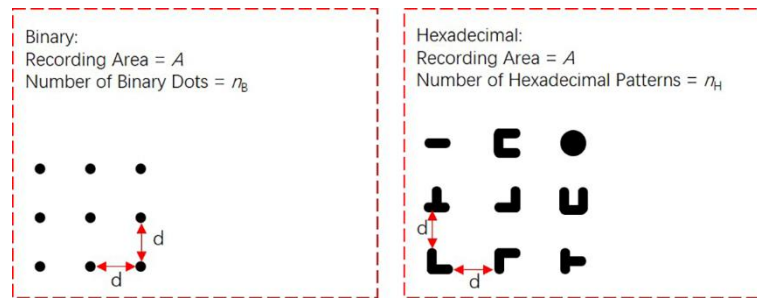


**Fig. S15** Schematic illustration of the data recorded in binary and hexadecimal formats.

For binary format, the recording density is  $\frac{1 \text{ bit} * n_B}{A}$ , while for hexadecimal format, since each hexadecimal pattern corresponds to 4 bits, the recording density is  $\frac{4 \text{ bit} * n_H}{A}$ . Obviously, the imaging quality (resolution/definition) of the camera plays an important role in determining the final data recording density, as it determines the total number of patterns can be recorded in a certain area.

Please note that the hexadecimal format is just an example of the algorithm-based “info-rich” format. Just like reading a painting, the amount of information we can get depends on our very way of thinking (i.e., the reading algorithm). We believe that by designing more sophisticated patterning and corresponding reading algorithm, the information density could be tremendously enhanced. Considering the advanced modern computational technology, the sophisticated algorithm could consume very small amount of computational resource.

Previously, gray scales and colors were also proposed to increase data recording density. Therefore, recording patterns with different gray scales or colors should be a very interesting idea to achieve high data recording density. However, precisely reading different gray scales and colors would require more sophisticated camera.

## References

1. W. Moerner, D. P. Fromm, *Rev. Sci. Instrum.* **2003**, *74*, 3597.
2. Y. Liu, C. B. Rauch, *Anal. Biochem.* **2003**, *317*, 76.
3. K. R. Hawkins, P. Yager, *Lab Chip* **2003**, *3*, 248.
4. P. Dedecker, B. Muls, A. Deres, H. Uji-i, J.-i. Hotta, M. Sliwa, J.-P. Soumillion, K. Müllen, J. Enderlein, J. Hofkens, *Adv. Mater.* **2009**, *21*, 1079.
5. H. Uji-i, A. Deres, B. Muls, S. Melnikov, J. Enderlein, J. Hofkens, in *Fluorescence of Supramolecules, Polymers, and Nanosystems*, Vol. 4 (Ed: M. N. Berberan-Santos), Springer Berlin Heidelberg, **2008**, 257.